2023 International Symposium on Nonlinear Theory and Its Applications
NOLTA2023, September 26-29, 2023, Catania and Online

Resource Allocation for Large Scale UAV Networks Using Coherent Ising Machine

Tsukumo Fujita[1], Aohan Li[2], Quang Vinh Do[3], Seon-Geun Jeong[3], Won-Joo Hwang[3]
Hiroki Takesue[4], Kensuke Inaba[4], Kazuyuki Aihara[5] and Mikio Hasegawa[1]

[1] Department of Electrical Engineering, Tokyo University of Science
6-3-1, Niijuku, Katushikaku, Tokyo 125-8585, Japan

[2] Graduate School of Informatics and Engineering, The University of Electro-Communications
1-5-1, Tyofugaoka, Tyofushi, Tokyo 182-8585, Japan

[3] Department of Biomedical Convergence Engineering, Pusan National University
Gyeongsangnam, Korea

[4] NTT Basic Research Laboratories, NTT Corporation, Atsugi, Kanagawa 243-0198, Japan

[5] International Research Center for Neurointelligence, The University of Tokyo
7-3-1, Hongou, Bunkyoku, Tokyo 113-0033, Japan

Email: 4322543@ed.tus.ac.jp, aohanli@ieee.org, quangdv@pusan.ac.kr,
wjdtjsrms11@pusan.ac.kr, wjhwang@pusan.ac.kr, fhiroki.takesue.km@hco.ntt.co.jp,
kensuke.inaba.yg@hco.ntt.co.jp, kaihara@g.ecc.utokyo.ac.jp, hasegawa@haselab.ee.kagu.tus.ac.jp

Abstract— Unmanned aerial vehicles (UAVs) are expected to be the next-generation wireless communication technology to enhance the service experience for mobile users on the ground. This article investigates wireless resource allocation in a large-scale UAV wireless network, where multiple UAVs communicate with ground users. To improve communication efficiency for all users in the presence of co-channel interference, we propose using a quantum annealing method for fast and accurate UAV-user association and resource allocation. We evaluate our proposed method through simulation using an optical Ising machine called Coherent Ising Machine (CIM) for optimization, and the simulation results show that our proposed method leads to better solutions than other methods.

1. Introduction

Unmanned aerial vehicles (UAVs) are being utilized in a wide range of communication scenarios to improve network coverage and performance due to their flexibility, versatility, and cost-effectiveness [1]. UAVs can also serve as aerial base stations to support high-efficiency spectrum communication in regions where ground station services are difficult to access. Therefore, UAV-based aerial platforms for providing wireless services have attracted a great deal of attention from academic and industrial communities. Despite these promising advantages, there are still many practical challenges associated with deploying UAVs for wireless communication.

Spectrum sharing is one of the major challenges with limited spectrum resources in UAV networks. However, sharing spectrum resources can cause interference, particularly in practical multi-UAV networks where dealing with co-channel interference becomes more complex than with ground-based systems. Some studies have been conducted on network performance optimization[2]. However, it is difficult to obtain optimal solutions quickly due to their computational complexity and cost. As a result, most existing research focuses on small-scale networks with only a few UAVs and users.

However, realistic UAV networks are larger and require faster optimization. Therefore, this study utilizes an optical Ising machine called CIM. CIM can optimize many large-scale problems quickly, and in previous research [3], various complex wireless communication systems were optimized using CIM-based optimization methods. While there is little research on the use of optical Ising machine in resource management for UAV networks, they can provide rapid and effective solutions to many optimization problems in wireless communication.

In this study, we optimized the wireless resource allocation with the aim of improving communication performance in a large-scale UAV network using CIM. Specifically, we investigated the UAV-user association, subchannel allocation, and power control problems for downlink transmission, taking into account the impact of co-channel interference on network performance.

ORCID iDs Tsukumo Fujita: 0009-0004-9075-9199, Aohan Li: 0000-0003-0618-4894, Quang Vinh Do: 0000-0002-6899-2347, Seon-Geun Jeong: 0000-0002-5926-6642, Won-Joo Hwang: 0000-0001-8398-564X, Hiroki Takesue: 0000-0003-1253-9049, Kensuke Inaba: 0000-0003-1227-4925, Kazuyuki Aihara: 0000-0002-4602-9816, Mikio Hasegawa: 0000-0001-5638-8002

2. Coherent Ising Machine

CIM [4] is a machine that can artificially reproduce the Ising model, a physical model of magnetic spin. Ising model consists of two states of magnetic spins: upward and downward. The spins are mutually coupled and are affected by interactions from other spins and from external magnetic fields. Here, the Ising Hamiltonian, which is the energy function of the Ising model, is expressed as follows.

$$E(\sigma) = -\frac{1}{2}\sum_{i=1}^{\mathcal{M}}\sum_{j=1}^{\mathcal{N}}\sum_{k=1}^{\mathcal{K}}\sum_{l=1}^{\mathcal{L}}\sum_{i'=1}^{\mathcal{M}}\sum_{j'=1}^{\mathcal{N}}\sum_{k'=1}^{\mathcal{K}}\sum_{l'=1}^{\mathcal{L}} J_{ijkl,i'j'k'l'}\sigma_{ijkl}\sigma_{i'j'k'l'} + \sum_{i=1}^{\mathcal{M}}\sum_{j=1}^{\mathcal{N}}\sum_{k=1}^{\mathcal{K}}\sum_{l=1}^{\mathcal{L}}\lambda_{ijkl}\sigma_{ijkl}, \tag{1}$$

where $\sigma_{ijkl} \in \{-1, +1\}$ is the spin direction, $J_{ijkli'j'k'l'}$ is the strength of the interaction, λ_{ijkl} is the strength of the external magnetic field. CIM can obtain the ground state of this Ising Hamiltonian. Hence, if we find J and λ for the optimization problem, we can quickly obtain the optimal solution. CIM needs to adjust the value of the pump rate, which is the magnitude of the amplitude of the light as the light pulse is amplified.

3. Problem Description

3.1. System model

We consider a large-scale UAV wireless network consisting of a macro base station (MBS) and M single-antenna UAVs operating as aerial base stations at a constant altitude. Figure 1 shows the system model in UAV networks. There are N ground users (GUs) that are randomly distributed within the circular geographical area of radius r_c of the MBS. We denote the sets of UAVs and users as $\mathcal{M} = \{1, \ldots, M\}$ and $\mathcal{N} = \{1, \ldots, N\}$, respectively. The total system bandwidth is divided into K orthogonal subchannels, denoted by $\mathcal{K} = \{1, \ldots, K\}$, and the subchannels allocated to the UAVs may overlap with each other. We assume the MBS is the network controller and that the UAVs can exchange information with the controller via perfect backhaul connections. Furthermore, the controller makes decisions about UAV-user association, subchannel assignment, and power control for downlink data transmissions.

The locations of UAV $m \in \mathcal{M}$ and GU $n \in \mathcal{N}$ in a three-dimensional space are denoted by $\boldsymbol{q}_m^{UAV} = (x_m, y_m, h)$ and $\boldsymbol{q}_n^{GU} = (x_n, y_n, 0)$, respectively, where h is the hovering altitude of the UAV. Similar to [5], we consider a probabilistic air-to-ground path-loss model, in which the communication channels between the UAVs and the GUs can be modeled as either line-of-sight (LoS) or non-line-of-sight (NLoS) links. More specifically, the probability that the channel between UAV m and GU n is LoS, denoted as $\rho_{m,n}^{LoS}$, is given by [6]

$$\rho_{m,n}^{LoS} = \frac{1}{1 + ae^{-b\left(\frac{180}{\pi}\arcsin\left(\frac{h}{d_{m,n}}\right) - a\right)}}, \tag{2}$$

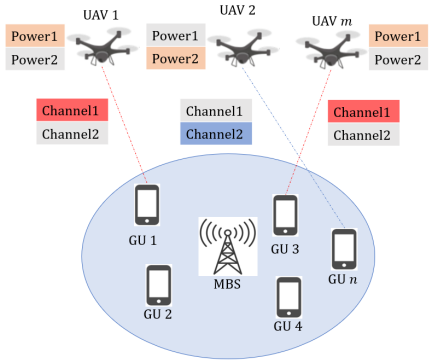

Figure 1: System model in UAV networks.

where a and b is the environment-dependent parameters, and $d_{m,n} = \sqrt{\|\boldsymbol{q}_m^{UAV} - \boldsymbol{q}_n^{GU}\|^2}$ is the distance between them. Hence, the probabilistic path loss is given by [5]

$$g_{m,n} = \left(\rho_{m,n}^{LoS} + \left(1 - \rho_{m,n}^{LoS}\right)\eta\right) g_{m,n}^{LoS}, \tag{3}$$

where $g_{m,n}^{LoS} = g_0 {d_{m,n}}^{-\epsilon_0}$ represent the free-space channel gain, g_0 is the channel gain at the reference distance $d_0 = 1$ m, ϵ_0 is the path-loss exponent, and η is the additional signal attenuation factor due to NLoS condition.

We denote as $\alpha_{m,n} \in \{0, 1\}$ the association variable between UAV m and GU n, i.e., if GU n is associated with UAV m, $\alpha_{m,n} = 1$; otherwise, $\alpha_{m,n} = 0$. In this work, we assume that each UAV can only associate with one GU at a time. Thus, the following constraint must hold

$$\sum_{n\in\mathcal{N}} \alpha_{m,n} \leq 1, \ \forall m \in \mathcal{M}, \tag{4}$$

Similarly, we denote as $\beta_m^k \in \{0, 1\}$ the subchannel assignment variable, i.e., if channel k is allocated to UAV m, $\beta_m^k = 1$, otherwise, $\beta_m^k = 0$. We have

$$\sum_{k\in\mathcal{K}} \beta_m^k \leq 1, \ \forall m \in \mathcal{M}, \tag{5}$$

which indicates that each UAV can only occupy a single subchannel at a time.

Moreover, the transmit power values by a UAV to communicate with its associated user can be selected in a list $\{P_1, P_2, \ldots, P_L\}$. We denote as $p_m^l \in \{0, 1\}$, $l \in \mathcal{L}$ the power level variable, i.e., if power level l is allocated to UAV m, $p_m^l = 1$, otherwise, $p_m^l = 0$. We have

$$\sum_{l\in\mathcal{L}} p_m^l \leq 1, \ \forall m \in \mathcal{M}, \tag{6}$$

which indicates that only one power level can be selected by UAV m at a time.

As a result, the signal-to-interference ratio (SIR) for the communication link between UAV m and GU n on subchannel k with power level l is given as:

$$\gamma_{m,n}^{k,l} = \frac{\alpha_{m,n}\beta_m^k p_m^l g_{m,n} P_l}{I_{m,n}^{k,l}}, \tag{7}$$

$I_{m,n}^{k,l}$ is the co-channel interference at UAV m caused by other UAVs operating on subchannel k, which is given as:

$$I_{m,n}^{k,l} = \sum_{m' \in \mathcal{M}, m' \neq m} \sum_{n' \in \mathcal{N}} \sum_{l' \in \mathcal{L}} \alpha_{m,n} \alpha_{m',n} \beta_m^k \beta_{m'}^k p_{m'}^{l'} g_{m',n} P_{l'}, \quad (8)$$

Thus, the SIR for UAV m, denoted as S_m, can be calculated as:

$$S_m = \sum_{n \in \mathcal{N}} \sum_{k \in \mathcal{K}} \sum_{l \in \mathcal{L}} \gamma_{m,n}^{k,l}, \ \forall m \in \mathcal{M}, \quad (9)$$

3.2. Problem Formulation

To summarize the above, the total SIR maximization problem can be formulated as follows:

$$\begin{aligned} \max_{\boldsymbol{\alpha},\boldsymbol{\beta},\boldsymbol{P}} \quad & S = \sum_{m \in \mathcal{M}} S_m, \\ s.t. \quad & \textstyle\sum_{n \in \mathcal{N}} \alpha_{m,n} \leq 1, \ \forall m \in \mathcal{M}, \\ & \textstyle\sum_{k \in \mathcal{K}} \beta_m^k \leq 1, \ \forall m \in \mathcal{M}, \\ & \textstyle\sum_{l \in \mathcal{L}} p_m^l \leq 1, \ \forall m \in \mathcal{M}, \\ & \alpha_{m,n} \in \{0,1\}, \ \beta_n^k \in \{0,1\}, \ p_m^l \in \{0,1\}, \end{aligned} \quad (10)$$

Moreover, although the objective function of the optimization problem was based on signal-to-interference ratio (SIR), signal to interference and noise power ratio (SINR) was used to evaluate the simulation results using white Gaussian noise, and the channel capacity was used as the evaluation metric. SINR can be calculated as follows:

$$SINR = \frac{\sum_{m \in \mathcal{M}} \sum_{n \in \mathcal{N}} \sum_{k \in \mathcal{K}} \sum_{l \in \mathcal{L}} \alpha_{m,n} \beta_m^k p_m^l g_{m,n} P_l}{\sum_{m \in \mathcal{M}} \sum_{n \in \mathcal{N}} \sum_{k \in \mathcal{K}} \sum_{l \in \mathcal{L}} I_{m,n}^{k,l} + k_B T B}, \quad (11)$$

Here, k_B is the Boltzmann constant, T is the temperature, and B is the bandwidth of the network. Furthermore, the channel capacity C can be obtained using Shannon's theorem as follows:

$$C = B \log (1 + SINR), \quad (12)$$

4. Solution

To solve optimization problems using a coherent Ising machine, it is necessary to transform the equation into a form like that shown in Eq.(1) and derive J and h. We introduce X_{mnkl} as the neuron shown in Eq.(13).

$$X_{mnkl} = \begin{cases} 1, & \text{if UAV } m \text{ associate with GU } n \\ & \text{using channel } k \text{ with power level } l, \\ 0, & \text{otherwise,} \end{cases} \quad (13)$$

Then, the objective function shown in Eq. (10) can be transformed to

$$\begin{aligned} \max_X & \sum_{m \in \mathcal{M}} \sum_{n \in \mathcal{N}} \sum_{k \in \mathcal{K}} \sum_{l \in \mathcal{L}} \frac{X_{mnkl} g_{m,n} P_l}{\sum_{m' \in \mathcal{M}, m' \neq m} \sum_{n' \in \mathcal{N}} \sum_{l' \in \mathcal{L}} X_{mnkl} X_{m'n'kl'} g_{m',n} P_{l'}} \\ & + \sum_{m' \in \mathcal{M}} \sum_{n' \in \mathcal{N}} \sum_{k' \in \mathcal{K}} \sum_{l' \in \mathcal{L}} \frac{X_{m'n'k'l'} g_{m',n'} P_{l'}}{\sum_{m \in \mathcal{M}, m \neq m'} \sum_{n \in \mathcal{N}} \sum_{l \in \mathcal{L}} X_{m'n'k'l'} X_{mnk'l} g_{m,n'} P_l}, \\ s.t. & \sum_{n \in \mathcal{N}} \sum_{k \in \mathcal{K}} \sum_{l \in \mathcal{L}} X_{mnkl} \leq 1, \ \forall m \in \mathcal{M}, \end{aligned} \quad (14)$$

Then, by taking the reciprocal and Kronecker delta, the objective function in Eq.(14) above can be transformed to

$$\begin{aligned} \min_X & \sum_{m \in \mathcal{M}} \sum_{n \in \mathcal{N}} \sum_{k \in \mathcal{K}} \sum_{l \in \mathcal{L}} \sum_{m' \in \mathcal{M}} \sum_{n' \in \mathcal{N}} \sum_{l' \in \mathcal{L}} \\ & \left(\frac{g_{m',n} P_{l'}}{g_{m,n} P_l} + \frac{g_{m,n'} P_l}{g_{m',n'} P_{l'}} \right) (1 - \delta_{mm'}) \delta_{kk'} X_{mnkl} X_{m'n'kl'}, \end{aligned} \quad (15)$$

Similarly, the constraints equation in Eq.(14) can be transformed to

$$\begin{aligned} & \sum_{m=1}^{\mathcal{M}} \left(\sum_{n=1}^{\mathcal{N}} \sum_{k=1}^{\mathcal{K}} \sum_{l=1}^{\mathcal{L}} X_{mnkl} - 1 \right)^2 \\ &= \sum_{m=1}^{\mathcal{M}} \sum_{n=1}^{\mathcal{N}} \sum_{k=1}^{\mathcal{K}} \sum_{l=1}^{\mathcal{L}} \sum_{m'=1}^{\mathcal{M}} \sum_{n'=1}^{\mathcal{N}} \sum_{k'=1}^{\mathcal{K}} \sum_{l'=1}^{\mathcal{L}} \delta_{mm'} (1 - \delta_{nn'} \delta_{kk'} \delta_{ll'}) X_{mnkl} X_{m'n'k'l'} \\ & - \sum_{m=1}^{\mathcal{M}} \sum_{n=1}^{\mathcal{N}} \sum_{k=1}^{\mathcal{K}} \sum_{l=1}^{\mathcal{L}} X_{mnkl} + M, \end{aligned} \quad (16)$$

Compared with Eq.(1), the connecting weights J of the Ising model and the external magnetic field λ is derived from Eq.(15) and Eq.(16).

$$\begin{aligned} w_{ijkl,i'j'k'l'} &= -2A (1 - \delta_{ii'}) \delta_{kk'} \left(\frac{g_{i',j} P_{l'}}{g_{i,j} P_l} + \frac{g_{i,j'} P_l}{g_{i',j'} P_{l'}} \right) \\ &\quad - 2B \delta_{ii'} \left(1 - \delta_{jj'} \delta_{kk'} \delta_{ll'} \right), \\ \theta_{ijkl} &= -B, \\ J_{ijkl,i'j'k'l'} &= \frac{w_{ijkl,i'j'k'l'}}{2}, \\ \lambda_{ijkl} &= \theta_{ijkl} - \frac{\sum_{i'=1}^{\mathcal{M}} \sum_{j'=1}^{\mathcal{N}} \sum_{k'=1}^{\mathcal{K}} \sum_{l'=1}^{\mathcal{L}} w_{ijkl,i'j'k'l'}}{2}, \end{aligned} \quad (17)$$

5. Numerical simulations

5.1. Parameter Settings

Table 1 and Figure 2 show the simulation parameter settings and the placement of UAVs and GUs within the cell radius for UAV networks. This UAV network environment was assumed with multiple ground users and UAVs in a 1000m radius MBS coverage area. That is, each UAV can connect to one of the 30 GUs in this coverage area at a time.

We compared our proposed method, CIM, to SA(Simulated Annealing) and SD(Steepest Descent) to evaluate its performance.

5.2. Simulation Results

Firstly, the results for channel capacity when the number of UAVs is varied are shown in Figure 3(a). The number of available channels was fixed at 5, and the number of UAVs was varied from 6 to 10 for the simulations. In addition, the number of CIM and SA iterations was all fixed to 1000. The results in Figure 3 (a) confirm that the solution derived

Table 1: Simulation Parameters in UAV Networks.

Parameter	Value
Number of ground users N	30
Number of UAVs M	10 (6,7,8,9,10)
Number of subchannels K	5 (4,5,6)
Service area radius r_c	1000 m
Environment-dependent parameters	$a = 10$, $b = 0.6$
Free-space channel gain g_0	−30 dB
Path-loss exponent ϵ_0	2
Additional signal attenuation factor η	0.2
Transmission power P_m	1 ∼ 10 W
UAVs' altitude h	100 m
Bandwidth of the entire network B	10 MHz

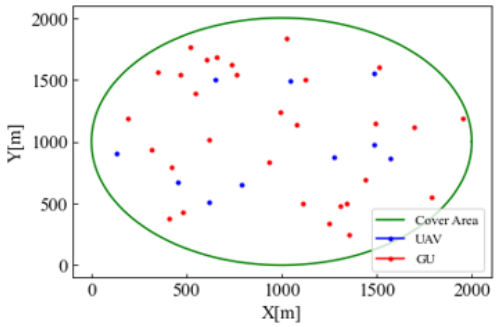

Figure 2: UAVs and GUs placement in UAV Networks.

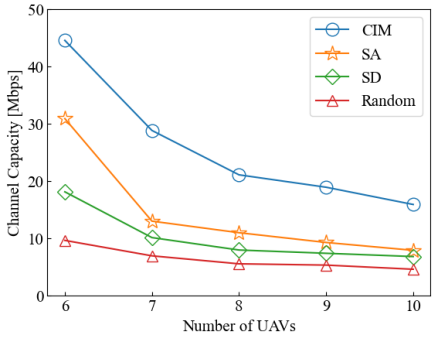

(a) Varying number of UAVs.

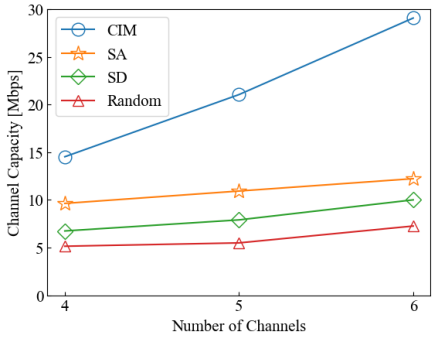

(b) Varying number of channels.

Figure 3: Total channel capacity for a varying number of UAVs or channels in UAV networks.

by CIM performs best for any number of UAVs. It can also be seen that the overall network channel capacity decreases as the number of UAVs increases. This is thought to be because the number of channels decreases, and as the number of UAVs increases, the effect of interference between channels increases.

Next, Figure 3(b) shows the results for channel capacity when the number of channels is varied. The number of UAVs was fixed at 10, and the number of channels was varied from 4 to 6 in the simulation. The results in Figure 3 (b) confirm that the solution derived by CIM has the best performance for any number of channels. These results also confirm that CIM performs better than the other comparison methods, especially when the number of UAVs is small and the number of channels is large.

6. Conclusion

In this paper, we investigate strategies for UAV-user association, subchannel allocation, and power control considering co-channel interference to enhance communication efficiency in large-scale UAV wireless networks. We formulate and transform this problem into an optimization problem to maximize the SIR in the UAV networks. Simulation results reveal that CIM yields the best-quality solution compared to other comparative methods.

References

[1] Z. Ullah et al, "Cognition in UAV-Aided 5G and Beyond Communications: A Survey," *IEEE TCCN*, vol.6, no.3, pp.872–891, 2020.

[2] L.Wang et al, "Enabling ultra-dense UAV-aided network with overlapped spectrum sharing: Potential and approaches," *IEEE Network*, vol.32, no.5, pp.85–91, 2018.

[3] K.Kurasawa et al, "A high-speed channel assignment algorithm for dense IEEE 802.11 systems via coherent Ising machine," *IEEE Wireless Communications Letters*, vol.10, no.8, pp.1682–1686, 2021.

[4] H.Takesue et al, "Simulating Ising spins in external magnetic fields with a network of degenerate optical parametric oscillators," *Physical Review Applied*, vol.13, no.5, pp.54–59, 2020.

[5] N. Babu et al, "Energy-Efficient 3-D Deployment of Aerial Access Points in a UAV Communication System," *IEEE Communications Letters*, vol.24, no.12, pp.2883–2887, 2020.

[6] A. Al-Hourani et al, "Optimal LAP altitude for maximum coverage," *IEEE Wireless Communications Letters*, vol.3, no.6, pp.569–572, 2014.